# Interval Estimation of Landslide Displacement Prediction Based on Time Series Decomposition and Long Short-Term Memory Network

## YIN XING[ID][1], JIANPING YUE[ID][1], AND CHUANG CHEN[ID][2]

[1]School of Earth Sciences and Engineering, Hohai University, Nanjing 211100, China
[2]College of Automation Engineering, Nanjing University of Aeronautics and Astronautics, Nanjing 211106, China

Corresponding author: Jianping Yue (yuejping@163.com)

**ABSTRACT** Interval estimation of landslide displacement prediction is significant for landslide early warning. The goal of this paper is to improve the accuracy of landslide displacement point prediction and quantify the uncertainties associated with the predicted values. To do so, a coupling prediction model based on double moving average (DMA) method and long short-term memory (LSTM) network is investigated. The DMA method is employed to decompose cumulative displacement of landslide into trend and periodic displacements, while the LSTM network is adopted to model and predict these two sub dis-placements. The sum of predicted sub displacements is considered as predicted cumulative displacement. Further, the probability estimation theory is utilized to derive confidence intervals that quantify the uncertainties of the point prediction. The proposed approach was validated on Baishuihe landslide in Three Gorges Reservoir area of China. Results show that the LSTM network performs better than support vector machine and Elman network, while the DMA decomposition method outperforms single moving average method. As a consequence, the coupling prediction model of DMA and LSTM network is a better solution for the point prediction of landslide displacement. Furthermore, the proposed probability estimation method can construct high-quality confidence intervals.

**INDEX TERMS** Landslide displacement prediction, interval estimation, deep learning, time series decomposition, Three Gorges Reservoir.

## I. INTRODUCTION

Landslides are severe natural calamities that threaten human life and property [1]–[5]. They occur frequently around the world. Landslide displacement is the most intuitive manifestation of landslide deformation. When the deformation reaches a certain degree, the landslide disaster is likely to occur. Therefore, the prediction of landslide displacement can be used to judge the evolution trend of landslide so as to realize early warning. However, landslide system usually presents complex nonlinear characteristics due to the complexity of local geological conditions and the randomness of external inducing factors. In this case, the landslide displacement has great uncertainties, presenting many difficulties for accurate landslide displacement prediction [6].

The associate editor coordinating the review of this manuscript and approving it for publication was Berdakh Abibullaev[ID].

Currently, the landslide displacement prediction has been a contentious issue.

The landslide displacement prediction approaches mainly invert inherent nonlinear dynamic evolution process of landslide by analyzing landslide displacement-time curve and monitoring information of various external influence factors. Following this idea, the nonlinear mapping relation between various influence factors and landslide displacement is first established, and then the evolution trend is predicted through extrapolation. The landslide displacement can be predicted by curve fitting techniques, such as Verhulst model, grey model, exponential smoothing model and so on [7]–[9]. With improvement of landslide monitoring techniques, the monitoring data become diversified and complicated. In recent years, many scholars have attempted to apply various advanced computational intelligence methods to landslide displacement prediction. For example, Du *et al.* [10]

**IEEE** *Access*

Y. Xing *et al.*: Interval Estimation of Landslide Displacement Prediction Based on Time Series Decomposition and LSTM Network

utilized single moving average (SMA) method to decompose landslide cumulative displacement into two sub displacements. After that, an artificial neural network was adopted to model and forecast the two sub displacements considering the external influence factors. Miao *et al.* [11] employed multiple algorithms to determine optimal support vector machine (SVM) model. Subsequently, the evolution trend of displacement was forecasted using the cubic polynomial model whereas the periodic component was forecasted using the optimized SVM model. Similarly, the particle swarm optimization (PSO) was adopted to optimize the extreme learning machine (ELM) with kernel, and the hybrid model was confirmed to have good prediction accuracy when predicting each displacement component decomposed by wavelet transform [12]. With piecewise time weighted gradient, Zhang *et al.* [13] proposed a modified regularized Elman network. The modified network was proven to allow improving the prediction accuracy of landslide displacement.

Unfortunately, the above studies have two shortcomings: first, these used models, which belong to shallow machine learning methods, are tough to excavate the inherent law between influence factors and landslide displacement; second, the above studies only focus on the deterministic values of displacement prediction without considering the uncertainties of the prediction. The first problem restricts the accuracy of landslide displacement prediction, while the second problem is very important for the later landslide treatment. To address the two problems, we introduce a deep learning model, so-called long short-term memory (LSTM) network, and theoretically derive the confidence intervals of landslide displacement prediction at a certain confidence level. The main highlights of this paper are as follows.

- *Coupling prediction approach*: The double moving average (DMA) first decomposes cumulative displacement into two stationary sequences and the LSTM network is employed to model and predict these two stationary sequences. Therefore, the coupling model of DMA and LSTM network can solve the problem of non-stationary cumulative displacement prediction.
- *High predictive accuracy with optimal network parameters*: The L2 regularization method is introduced to solve the LSTM network over-fitting problem, while the Adam algorithm is introduced to promote the network convergence. Thus, the prediction accuracy of LSTM network is improved.
- *High-quality confidence intervals*: According to the probability estimation theory, the confidence intervals of landslide displacement are derived, which provides a reference for formulating a reasonable landslide treatment plan.

The remainder of this paper is structured as follows. Section II is devoted to describing the fundamental theory of LSTM network and interval estimation approach. Section III presents the prediction scheme of landslide displacement with interval estimation, including the DMA-based time series decomposition and the coupling model-based prediction process.

In Section IV, a realistic landslide case is used to validate the effectiveness and superiority of the landslide prediction scheme. To conclude, Section V summarizes the conclusions and prospects for the next step.

## II. LSTM NETWORK-BASED INTERVAL ESTIMATION APPROACH

### A. LSTM NETWORK

Recurrent neural network (RNN) is an active approach for dealing with dynamic time series [14]–[20]. As a special RNN, LSTM network [21] allows learning over long time sequences and keeping memory, addressing the problem of gradient disappearance through improving the traditional RNN neurons.

Fig.1 shows the sketch of LSTM network architecture. It contains three functional gates: input, output and forget. The input gate decides which information from outside is stored, while the output gate regulates the output of important information within the network. The forget gate is able to discard some redundant information. The three gates cooperate with each other to conduct the data processing. This process can be described mathematically as follows [22]–[24]:

$$f_t = \text{sig}\left(W_f \cdot [h_{t-1}, \ x_t] + b_f\right) \tag{1}$$

$$i_t = \text{sig}\left(W_i \cdot [h_{t-1}, \ x_t] + b_i\right) \tag{2}$$

$$C_t = f_t * C_{t-1} + i_t * \tanh\left(W_C \cdot [h_{t-1}, \ x_t] + b_C\right) \tag{3}$$

$$o_t = \text{sig}\left(W_o \cdot [h_{t-1}, \ x_t] + b_o\right) \tag{4}$$

$$h_t = o_t * \tanh(C_t) \tag{5}$$

where $x_t$ and $h_t$ denote the input and output at current time step, respectively; $h_{t-1}$ and $C_{t-1}$ are the output and cell memory at previous time step, respectively; $(W_f, W_i, W_C, W_o)$ and $(b_f, b_i, b_C, b_o)$ are the weight matrices and bias vectors of the forget gate, input gate, cell state layer and output gate, respectively; $f_t$, $i_t$ and $o_t$ are the activation vectors of the forget, input and output gates, respectively; "sig" and "tanh" denote the sigmoid function and hyperbolic tangent function, respectively; $[\cdot, \ \cdot]$ denotes the splicing of two vectors; "$\cdot$" and "$*$" mean the matrix multiplication and the element-wise multiplication, respectively.
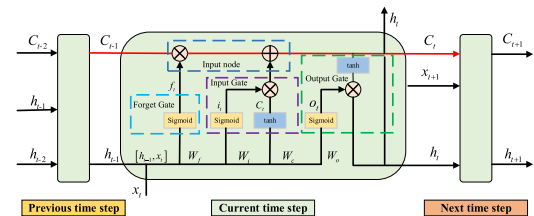


**FIGURE 1.** Sketch of LSTM network architecture.

When constructing the LSTM network, two crucial problems, which have a negative impact on prediction accuracy, need to be addressed. The first problem is the slow convergence speed of the network. The traditional gradient decent methods, such as the mini-batch gradient descent and

Y. Xing *et al.*: Interval Estimation of Landslide Displacement Prediction Based on Time Series Decomposition and LSTM Network

IEEE *Access*

stochastic gradient descent, are unable to ensure the rapid convergence. The second problem is how to void the over-fitting phenomenon. Currently, the two problems have been well addressed. With regard to the slow convergence speed of the network, the use of "Adam" method [25] is proposed to promote network convergence. Meanwhile, to void the over-fitting of the network, the use of "L2 regularization" method [26] is proposed to reduce the network complexity by reducing the size of network parameter values. Therefore, in this paper, we introduce the "Adam" and "L2 regularization" methods to assist the construction of LSTM network.

### B. INTERVAL ESTIMATION

The deterministic prediction values of landslide displacement can be obtained using the LSTM network. If the confidence intervals of landslide displacement can be known, it is of great engineering significance for comprehensive landslide treatment. To quantify the uncertainties associated with the predicted values, we derive the confidence intervals in the context of the LSTM network. The main derivation process is described as follows.

First of all, according to the fundamental theory of LSTM network, the prediction model can be expressed as

$$y = \hat{f}(x) + \xi \tag{6}$$

where $x$, $y$ and $\xi$ denote the input, output and random variable, respectively. Suppose $\xi$ is independent of $x$, and then the $i$-th $(i = 1, \cdots, M)$ random variable is given by

$$\xi_i = y_i - \hat{f}(x_i) \tag{7}$$

where $M$ is the number of input samples. In general, $\xi$ follows Gauss distribution or Laplace distribution with zero mean, and in most cases, it follows the Laplace distribution [27]. The density function of the Laplace distribution with parameter $\sigma$ is given by

$$p(z) = \frac{1}{2\sigma} exp(-\frac{|z|}{\sigma}). \tag{8}$$

Next, the maximum likelihood estimation method is used to estimate the parameter $\sigma$. Here, the maximum likelihood function with $\sigma$ is

$$L(\sigma; \xi) = (\frac{1}{2\sigma})^M exp(-\frac{|\xi_1| + |\xi_2| + \cdots + |\xi_M|}{\sigma}). \tag{9}$$

Let $\frac{\partial lnL}{\partial \sigma} = 0$, and then the estimated value of $\sigma$ is obtained as

$$\hat{\sigma} = \frac{1}{M} \sum_{i=1}^{M} |\xi_i|. \tag{10}$$

Given a confidence level $p_0$, i.e. $P(\hat{y} - \Delta \leq y \leq \hat{y} + \Delta) = p_0$, the interval $\Delta$ is obtained as

$$p_0 = \int_{-\Delta}^{\Delta} p(\xi)d\xi = 1 - exp(-\frac{\Delta}{\hat{\sigma}}),$$
$$\Delta = \left| \hat{\sigma} ln(1 - p_0) \right|. \tag{11}$$

Therefore, the output intervals of the LSTM network at the certain confidence level $p_0$ are $\left[ \hat{y} - \left| \hat{\sigma} \ln(1 - p_0) \right|, \hat{y} + \left| \hat{\sigma} \ln(1 - p_0) \right| \right]$.

## III. PREDICTION SCHEME OF LANDSLIDE DISPLACEMENT WITH INTERVAL ESTIMATION

### A. TIME SERIES DECOMPOSITION

A fact is that the local geological conditions and the external inducing factors together lead to the generation and evolution of landslide displacement [28]. Under the control of the local geological conditions, e.g. the geomorphology and the geological structure, the displacement shows an approximate monotonic increasing function on a large time scale. In addition, the reservoir water level, rainfall intensity and other external factors make the displacement show an approximate periodic function on a small time scale. Thus, the cumulative displacement, denoted by $c(t)$, shows a step-like behavior with time and can be decomposed as:

$$c(t) = \mu(t) + \rho(t) \tag{12}$$

where $\mu(t)$ and $\rho(t)$ denote the trend and periodic displacements at $t$ time, respectively.

DMA is a simple but effective method for time series decomposition [29]. It allows decomposing original cumulative displacement into trend and periodic displacements. Unlike the SMA method [10], the DMA method can extract smoother trend displacement which is suitable for modeling. First of all, the trend displacement, denoted by $\mu_1(t)$, is extracted by the SMA method and is given by

$$\mu_1(t) = \frac{c(t - n + 1) + c(t - n + 2) + \cdots + c(t)}{n} \tag{13}$$

where $n$ represents the step number and satisfies $n < t$. After that, the DMA is applied to the $\mu_1(t)$ and obtains the expected trend displacement, denoted by $\mu_2(t)$. The process can be expressed as

$$\mu_2(t) = \frac{\mu_1(t - n + 1) + \mu_1(t - n + 2) + \cdots + \mu_1(t)}{n}. \tag{14}$$

Based on this, the $\rho(t)$ is obtained as

$$\rho(t) = c(t) - \mu_2(t). \tag{15}$$

### B. PREDICTION PROCESS

The cumulative displacement of landslide is a non-stationary sequence. If the LSTM network is used directly to model, it is tough to find the inherent law between the influence factors and landslide displacement. A good idea is to decompose the non-stationary sequence into several stationary sequences. Here, the DMA method is adopted to decompose the cumulative displacement, and the trend and periodic displacements are obtained. Next, the LSTM network is used to model and predict these two sub displacements, respectively. Thus, the sum of predicted components is the predicted cumulative
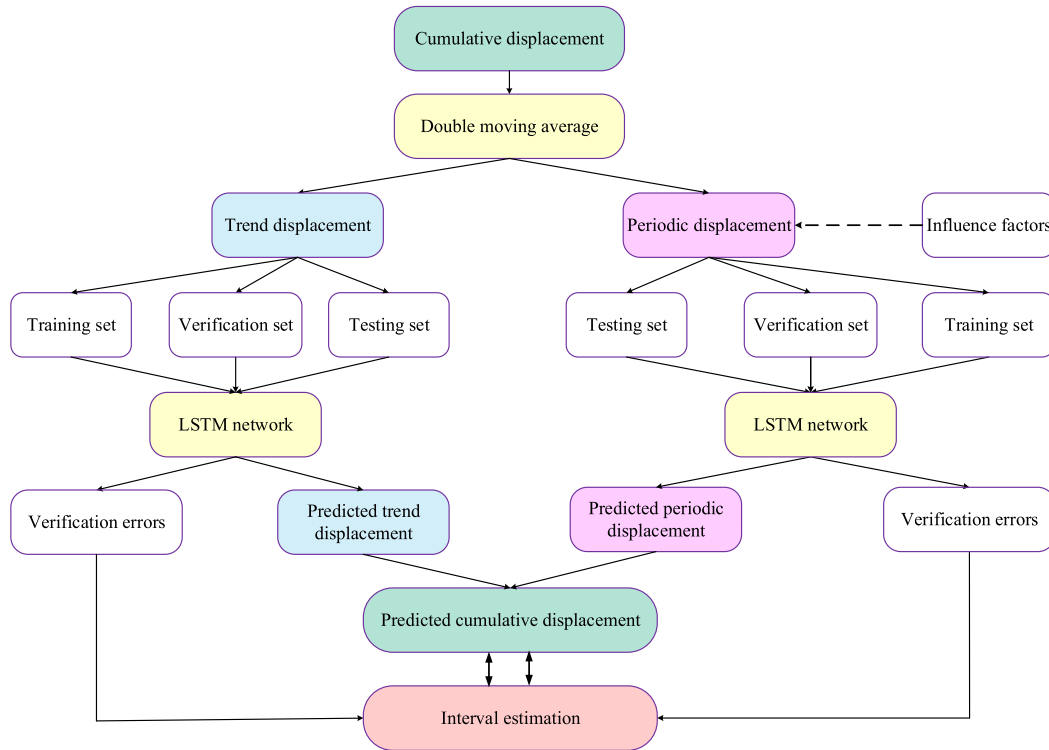
**FIGURE 2.** Prediction process of landslide cumulative displacement.

displacement. On the other hand, for obtaining the confidence intervals, a verification set is set to estimate the value of parameter $\sigma$. Fig. 2 shows the prediction process of landslide cumulative displacement, and the main steps of the process are presented as follows.

*Step 1:* Use the DMA method to decompose the cumulative displacement and gain two displacement components: trend and periodic.

*Step 2:* Construct the training, verification and testing sets corresponding to each displacement component.

*Step 3:* Use the LSTM network to learn from each training set and bring the samples of the verification and testing sets into the trained LSTM network to produce the prediction results.

*Step 4:* Add the prediction results of the testing sets together and gain the cumulative displacement.

*Step 5:* Calculate the prediction errors of the verification sets, and the final confidence intervals are obtained by Eqs. (10) and (11).

In the field of landslide displacement prediction, two model evaluation indicators are often used. The first one is the root mean square error (RMSE), and the other is the mean absolute error (MAE). They reflect the performance of the model from different perspectives. It is recognized that the model having lower values of RMSE and MAE implies better prediction performance. For more information about them, see the literature [30], [31]. In this paper, we also adopt these two indicators to evaluate our model, and the RMSE and

MAE can be expressed as

$$RMSE = \sqrt{\frac{1}{N}\sum_{i=1}^{N}(s_i - \hat{s}_i)^2} \qquad (16)$$

$$MAE = \frac{1}{N}\sum_{i=1}^{N}\left|s_i - \hat{s}_i\right| \qquad (17)$$

where $s_i$ and $\hat{s}_i$ denote the actual observation value and the prediction value, respectively; $N$ denotes the prediction sample number.

## IV. CASE STUDY
### A. BAISHUIHE LANDSLIDE
The landslide is situated in Zigui County, Yichang City, Hubei Province, China (110°32′ 09″ E, 31°01′ 34″ N). The distance between it and the Three Gorges Dam is about 56 km. Fig. 3 shows its geological section. It is observed that the landslide is a monoclinic downward slope with main direction of NE20°. Also, the average thickness of the landslide is about 30 m, and the volume is about $1.26 \times 10^7$ m³. For the elevation, it ranges from 75 to 390 m. The front edge of the landslide is submerged below the reservoir, while the trailing edge is bounded by the interface between the rock and soil.

Two sliding surfaces are observed at different depths, i.e. initial and secondary sliding surfaces. The initial sliding surface depth exceeds 30 m, whereas the secondary sliding surface depth ranges from 12 to 21.5 m. This may be
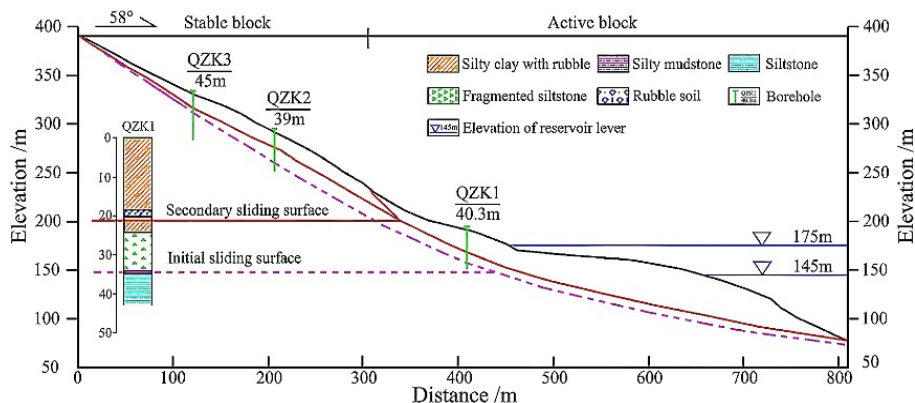
Y. Xing *et al.*: Interval Estimation of Landslide Displacement Prediction Based on Time Series Decomposition and LSTM Network

IEEE *Access*



**FIGURE 3.** Geological section of Baishuihe landslide [13].

explained that because of the complex geological conditions and large volume of the Baishuihe landslide, more energy would be required to completely destroy along the initial sliding surface [13].

Since June 2003, professional monitoring of Baishuihe landslide has been carried out. Currently, many GPS monitoring detectors have been set up on the landslide body, and the specific distribution is depicted in Fig. 4. According to the monitoring data, it is known that the landslide deformation mainly occurs in the active block area, which is defined as the early warning area, while the remaining deformation is not obvious. There are six GPS monitoring points in the early warning area, i.e. ZG093, ZG118, XD-01, XD-02, XD-03 and XD-04. Compared with the other five GPS monitoring points, the ZG118 monitoring point has two advantages: one is that it has the most complete data due to the longest monitoring period; the other is that it is situated in the central section of the landslide body, which can better reflect the entire process of landslide evolution. Therefore, this paper select the data of ZG118 monitoring point for research.
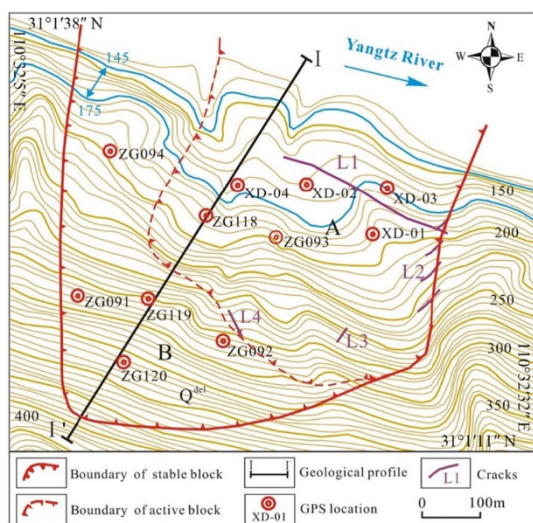


**FIGURE 4.** Distribution of monitoring points in Baishuihe landslide [13].
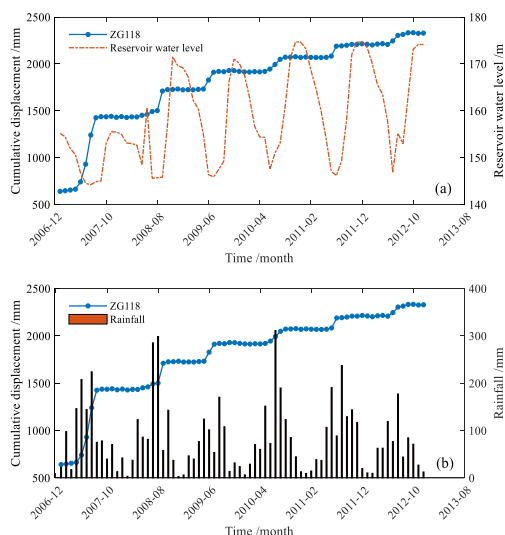


**FIGURE 5.** Monitoring curves of cumulative displacement, reservoir water level (a) and rainfall (b).

Fig. 5 shows the monitoring curves of Baishuihe landslide from January 2007 to December 2012. It can be seen that from January 2007 to September 2008, the reservoir water level varies from 145 to 155 m. During its rising period, the cumulative displacement is relatively stable with the maximum growth rate of only 19 mm per month. As the reservoir water level first drops from 155 m to 145 m, the cumulative displacement increases abruptly, and the maximum displacement growth rate reaches 334 mm per month (July 2007). This can be interpreted as the result of strong external inducing factors: the rainfall during flood season and the significant drop in reservoir water level. Subsequently, these two inducing factors weaken, and the cumulative displacement gradually restores to a stable state. From October 2008 to December 2012, the reservoir water level fluctuates periodically from 145 to 175 m, and the cumulative displacement continues to increase in a step-like manner. The maximum displacement growth rate of monitoring points occurs in the period of reservoir water level decline or low water level.

**IEEE** *Access*

Y. Xing *et al.*: Interval Estimation of Landslide Displacement Prediction Based on Time Series Decomposition and LSTM Network

The maximum displacement growth rates in four years are 99 (2009), 74 (2010), 84 (2011) and 63 mm per month (2012), respectively. With the long-term regulation of reservoir water level, the landslide has undergone the stress adjustment. Thus, it adapts to the new regulation mode of reservoir water level. Consequently, the displacement growth gradually tends to be stable.

### B. CUMULATIVE DISPLACEMENT DECOMPOSITION
Fig. 6 shows the decomposition results of cumulative displacement using the DMA method. Apparently, the cumulative displacement shows a non-stationary characteristic, whereas the decomposed sequences are relatively stable.
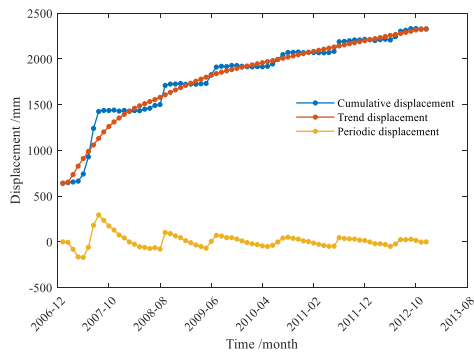


**FIGURE 6.** Decomposition results of cumulative displacement using DMA method.

In the experiment, the LSTM layer is designated as 200 hidden units. To prevent the gradients from exploding, the number of epochs and the gradient threshold of ''Adam'' algorithm are set to 250 and 1, respectively. According to each displacement component, the training, verification and testing sets are constructed, respectively. Specifically, the data from January 2007 to December 2010 are taken as the training set, while the data from January to December 2012 as the testing set. Also, the verification set, i.e. the data from January to December 2011, is divided to estimate the parameter $\sigma$.

To highlight the prediction performance of LSTM network, the existing landslide displacement prediction models: SVM and Elman network, are used for comparison. Further, the optimal model parameters of SVM and Elman network are determined by PSO algorithm, where the particle number is 20, the maximum iteration number is 200, both learning factors are 1.5 and the inertia weight is 1.

### C. DISPLACEMENTS PREDICTION
#### 1) TREND DISPLACEMENT PREDICTION
For predicting the trend displacement of the next month, the trend displacement of the previous month is used as the model input. For the use of this methodology, the basic assumption is, there is no strain softening along the sliding surface soils. When considerable strain softening exists along slip surfaces, abruptly, very large displacement may occur due both rainfall and earthquakes [32]–[35]. In this event,

this displacement cannot be predicted and is not related to previous displacement data.

Fig. 7 shows the prediction results of trend displacement using the LSTM, SVM and Elman models. It can be seen that before September 2012, the predicted values of LSTM network are closer to the actual values, followed by the Elman network and SVM, while the Elman network and SVM outperform the LSTM network from September to December 2012. Overall, the LSTM network performs well.
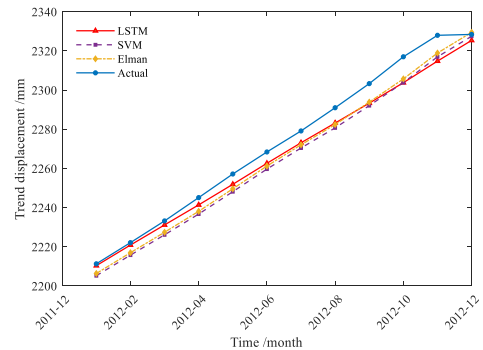


**FIGURE 7.** Prediction results of trend displacement using LSTM, SVM and Elman models.

Table 1 reports the RMSE and MAE values of the three models. The RMSE value of the LSTM network is 7.28 mm, lower than 8.94 mm of the SVM and 7.45 mm of the Elman network. Besides, the MAE value of the LSTM network is 6.02 mm, lower than 8.42 mm of the SVM and 7.01 mm of the Elman network. These results show that for the trend displacement prediction, the LSTM network outperforms the SVM and Elman network.

**TABLE 1.** Prediction errors of trend displacement using LSTM, SVM and Elman models (mm).

| Model | RMSE | MAE |
|-------|------|-----|
| LSTM | 7.28 | 6.02 |
| SVM | 8.94 | 8.42 |
| Elman | 7.45 | 7.01 |

#### 2) PERIODIC DISPLACEMENT PREDICTION
The selection of influence factors is crucial for the accuracy of periodic displacement prediction. First of all, rainfall is the main factor of landslide deformation and destruction in the Three Gorges Reservoir area. The impact of rainfall is embodied in the following two dimensions: 1) the landslide structure is changed by scouring the landslide surface; 2) the volume density, the strength parameters of the sliding zone soil and the dynamic and hydrostatic pressure of the landslide are changed through infiltration [36]. The rainfall infiltration occurs in a relatively slow process. The effective rainfall from one month to two months before the occurrence of landslide has a great impact on landslide deformation. Fig. 8 shows the curves of the periodic displacement of ZG118 monitoring point, maximum rainfall during current month, cumulative rainfall during current month and cumulative rainfall during
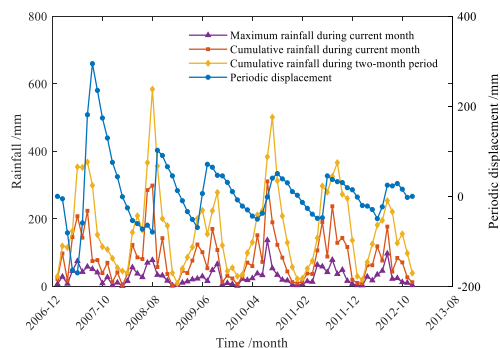
Y. Xing *et al.*: Interval Estimation of Landslide Displacement Prediction Based on Time Series Decomposition and LSTM Network

IEEE*Access*



**FIGURE 8.** Relationship between periodic displacement and rainfall.

two-month period. It is observed that the regularity of periodic displacement fluctuation is consistent with that of the three factors.

Secondly, the influence of reservoir water level fluctuation on landslide deformation is mainly reflected in two dimensions: 1) it causes the loading and unloading of the dry-wet cycle of the landslide, which in turn affects the physical and mechanical properties of the rock and soil; 2) it changes the seepage field inside the landslide, which in turn affects the mechanical effects inside and outside the landslide [37]. Under the same condition of reservoir water level change, the different initial elevations of reservoir water level have different influences on the landslide deformation. In addition, the reservoir water level change has a certain hysteresis impact on the landslide deformation. Therefore, the reservoir water level during current month (Fig. 5), the change in reservoir water level during current month and the change in reservoir water level during two-month period are selected to characterize the influence factors of reservoir water, as shown in Fig. 9. Intuitively, the regularity of periodic displacement fluctuation is consistent with that of the three factors.
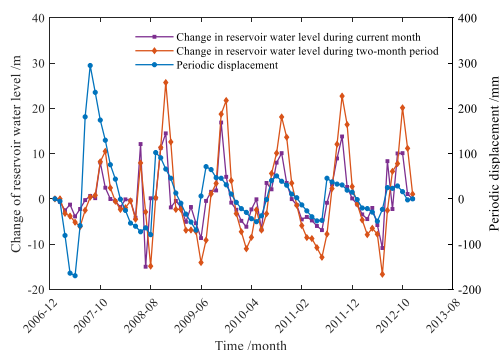


**FIGURE 9.** Relationship between periodic displacement and changes of reservoir water level.

Finally, under the same external excitation, the displacement responses of landslides with different deformation states are different. While the landslide is in a stable state, even strong external factors can hardly cause large-scale deformation of the landslide. However, for the landslide in a critical state, the slight disturbance may destroy the original balance

of the landslide system, thereby causing landslide deformation [38]. Therefore, the influence factors of landslide deformation state can be characterized by the cumulative displacement increment during current month, the cumulative displacement increment during two-month period and the cumulative displacement increment during three-month period, as shown in Fig. 10.
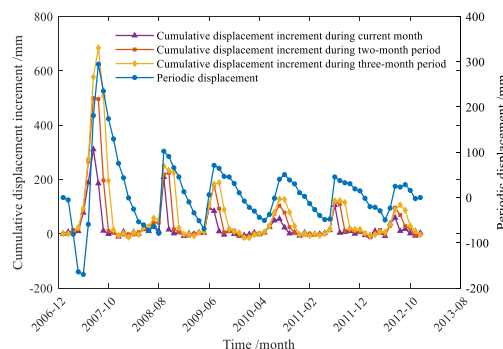


**FIGURE 10.** Relationship between periodic displacement and cumulative displacement increment.

In summary, the following nine influence factors are extracted for the periodic displacement prediction in this paper, as shown in Table 2. Following the work of [37], [39], the grey relational grades (GRG) between the nine influence factors and the periodic displacement of landslide exceed 0.6. Thus, the nine influence factors are considered to be closely related to the periodic displacement.

**TABLE 2.** List of influence factors.

| Index | Description |
|---|---|
| 1 | Maximum rainfall during current month |
| 2 | Cumulative rainfall during current month |
| 3 | Cumulative rainfall during two-month period |
| 4 | Reservoir water level during current month |
| 5 | Change in reservoir water level during current month |
| 6 | Change in reservoir water level during two-month period |
| 7 | Cumulative displacement increment during current month |
| 8 | Cumulative displacement increment during two-month period |
| 9 | Cumulative displacement increment during three-month period |

Next, the nine influence factors are fed into LSTM, SVM and Elman models, respectively. Fig. 11 shows the prediction results of periodic displacement. It is observed that the predicted values of LSTM network from January to December 2012 are approaching the actual values. Regarding the SVM, the prediction results for the period from August to October 2012 are not satisfactory. With regard to the Elman network, the predicted values deviate significantly from the actual values from June to August 2012. This may be due to the sudden and drastic changes in rainfall (Fig. 8) or reservoir water level (Fig. 9) between June and October 2012, whereas the SVM and Elman models are unable to accommodate the changes.

Table 3 reports the RMSE and MAE values of the three models. The RMSE value of the LSTM network is 6.92 mm, lower than 15.10 mm of the SVM and 27.88 mm of the
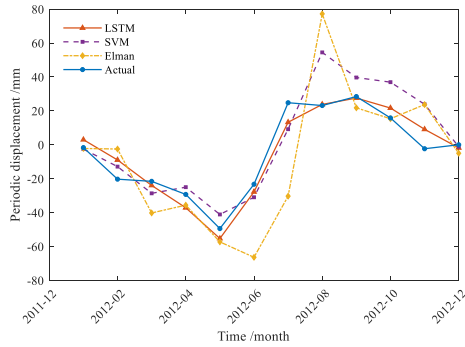
**FIGURE 11.** Prediction results of periodic displacement using LSTM, SVM and Elman models.

**TABLE 3.** Prediction errors of periodic displacement using LSTM, SVM and Elman models (mm).

| Model | RMSE | MAE |
|-------|------|------|
| LSTM | 6.92 | 5.73 |
| SVM | 15.10 | 11.85 |
| Elman | 27.88 | 20.12 |

Elman network. Besides, the MAE value of the LSTM network is 5.73 mm, lower than 11.85 mm of the SVM and 20.12 mm of the Elman network. These results show that for the periodic displacement prediction, the LSTM network outperforms the SVM and Elman network.

### 3) CUMULATIVE DISPLACEMENT PREDICTION

The predicted results of cumulative displacement are gained by reconstructing the predicted trend and periodic displacements, as shown in Fig. 12 (a). Compared with Fig. 11, the cumulative displacement curve is similar to the periodic displacement curve, which indicates that the prediction accuracy of periodic displacement has a crucial impact on that of the cumulative displacement. Compared with the SVM and Elman network, the predicted values of cumulative displacement using the LSTM network are closer to the actual values of cumulative displacement.

Also, to illustrate the superiority of the DMA method, the SMA method is used for comparison, as shown in Fig. 12 (b). Apparently, the predicted values of LSTM network from January to December 2012 are very close to the actual displacement values. Compared with Fig. 12 (a), regardless of the LSTM network, SVM or Elman network, the predicted values based on the DMA decomposition method appear to be better than those based on the SMA decomposition method, especially for the period from August to December 2012.

From a quantitative point of view, Table 4 reports the RMSE and MAE values of the three models under the DMA and SMA decomposition methods. First of all, for the DMA decomposition, the RMSE and MAE of the LSTM network are 9.38 mm and 8.39 mm, respectively, lower than those of the SVM and Elman network. Regarding the SMA decomposition, the RMSE and MAE of the LSTM network are
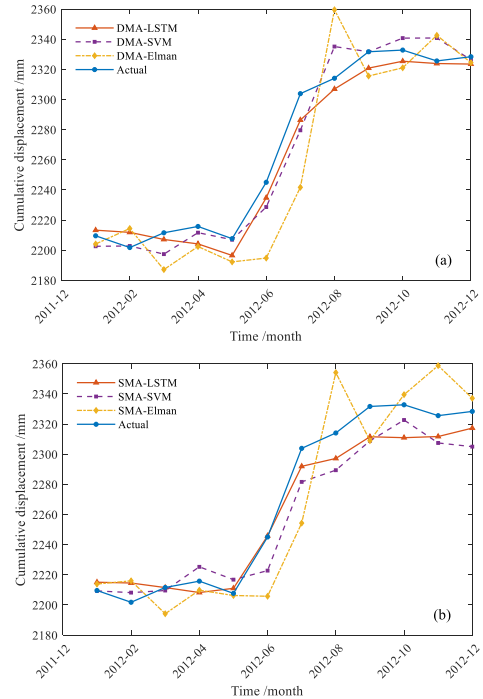


**FIGURE 12.** Prediction results of cumulative displacement using LSTM, SVM and Elman models under DMA (a) and SMA (b) decompositions.

**TABLE 4.** Prediction errors of cumulative displacement using LSTM, SVM and Elman Models under the DMA and SMA decomposition methods (mm).

| Model | DMA decomposition | | SMA decomposition | |
|-------|------|------|------|------|
| | RMSE | MAE | RMSE | MAE |
| LSTM | 9.38 | 8.39 | 12.53 | 10.47 |
| SVM | 12.48 | 9.49 | 16.63 | 14.25 |
| Elman | 29.38 | 23.16 | 25.68 | 20.31 |

12.53 mm and 10.47 mm, respectively, lower than those of the SVM and Elman network. These results reveal that the LSTM network outperforms the SVM and Elman network. Secondly, the Elman network, which is the worst of the three models, is set aside. In this event, it is concluded that regardless of the LSTM network or SVM, the prediction accuracy of the DMA decomposition method is higher than that of the SMA decomposition method, indicating that the DMA method outperforms the SMA method. Therefore, it makes sense to believe that the proposed coupling prediction model, namely DMA decomposition and LSTM network, is optimal in terms of prediction accuracy.
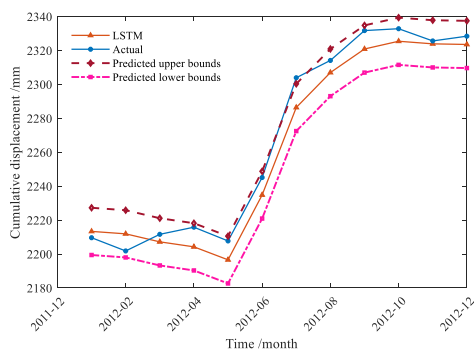
### D. CONFIDENCE INTERVALS

In this section, we aim to give the confidence intervals. Table 5 reports the prediction results of trend and periodic displacements using the proposed coupling model on the verification set. It can be calculated that the average absolute total error of cumulative displacement prediction is 8.65 mm. Thus, according to the Eq. (10), the parameter can be estimated as $\hat{\sigma} = 8.65$. Given the confidence level $p_0 = 0.8$, the interval is obtained as $\Delta = 13.92$ mm according to the Eq. (11).

Y. Xing et al.: Interval Estimation of Landslide Displacement Prediction Based on Time Series Decomposition and LSTM Network

IEEE Access

**TABLE 5.** Prediction results of trend and periodic displacements using LSTM network (mm).

| Date | Actual trend displacement | Predicted trend displacement | Trend error | Actual periodic displacement | Predicted periodic displacement | Periodic error | Total error |
|---|---|---|---|---|---|---|---|
| 2011-01 | 2070.98 | 2070.98 | 0.00 | 2.42 | -0.19 | -2.61 | -2.61 |
| 2011-02 | 2083.11 | 2083.32 | 0.21 | -13.41 | -11.59 | 1.82 | 2.03 |
| 2011-03 | 2095.14 | 2095.38 | 0.24 | -26.59 | -20.91 | 5.68 | 5.92 |
| 2011-04 | 2107.00 | 2107.12 | 0.12 | -39.60 | -29.26 | 10.34 | 10.46 |
| 2011-05 | 2118.84 | 2118.47 | -0.37 | -48.74 | -56.25 | -7.51 | -7.88 |
| 2011-06 | 2130.84 | 2129.46 | -1.38 | -47.54 | -56.92 | -9.38 | -10.76 |
| 2011-07 | 2143.13 | 2140.15 | -2.98 | 45.47 | 21.70 | -23.77 | -26.75 |
| 2011-08 | 2154.73 | 2150.63 | -4.1 | 37.37 | 31.90 | -5.47 | -9.57 |
| 2011-09 | 2166.25 | 2160.60 | -5.65 | 32.55 | 36.15 | 3.60 | -2.05 |
| 2011-10 | 2177.69 | 2170.18 | -7.51 | 30.61 | 34.29 | 3.68 | -3.83 |
| 2011-11 | 2189.05 | 2179.41 | -9.64 | 19.15 | 22.49 | 3.34 | -6.30 |
| 2011-12 | 2200.30 | 2188.34 | -11.96 | 14.70 | 10.99 | -3.71 | -15.67 |

Fig. 13 shows the confidence intervals of the landslide cumulative displacement. The confidence intervals refer to the area composed of prediction upper and lower bounds. It can be seen that only the actual value of landslide cumulative displacement in July 2012 is not within the area, while the other actual values of landslide cumulative displacement are within the area. This applies that the proposed estimation method is able to construct high-quality confidence intervals. Of course, as the confidence level increases, the confidence intervals will increase. In practice, the disaster prevention officer can formulate a reasonable landslide treatment plan according to the confidence intervals.



**FIGURE 13.** Confidence intervals of cumulative displacement using DMA-LSTM network.

## V. CONCLUSION

In this work, a coupling prediction model of DMA decomposition and LSTM network has been developed for the landslide displacement. The case study on Baishuihe landslide in the Three Gorges Reservoir area of China reveals the effectiveness and superiority.

The use of the DMA, which is a simple but effective time series decomposition method, is proposed to decompose the cumulative displacement of landslide. Compared with the SMA method, the DMA can extract the total trend reflecting the landslide displacement evolution more thoroughly. The use of LSTM network, which is an advanced predictor that can make full use of landslide historical information,

is proposed to perform the prediction tasks. Compared with two benchmark prediction models: SVM and Elman network, the model improves the prediction accuracy. Besides, considering the uncertainties of prediction results, the confidence intervals are derived according to the probability estimation theory. The proposed estimation method can construct high-quality confidence intervals. All in all, the above work provides valuable information for landslide early warning and control.

One limitation of the proposed method is that there are many parameters to be trained in the LSTM network, resulting in longer computing time. The focus of future work is to improve the network structure or parameter training method.

## REFERENCES

[1] C. Lian, Z. Zeng, W. Yao, H. Tang, and C. L. P. Chen, "Landslide displacement prediction with uncertainty based on neural networks with random hidden weights," *IEEE Trans. Neural Netw. Learn.Syst.*, vol. 27, no. 12, pp. 2683–2695, Dec. 2016.

[2] P. Jiang and J. Chen, "Displacement prediction of landslide based on generalized regression neural networks with K-fold cross-validation," *Neurocomputing*, vol. 198, pp. 40–47, Jul. 2016.

[3] C. Lian, Z. Zeng, W. Yao, and H. Tang, "Multiple neural networks switched prediction for landslide displacement," *Eng. Geol.*, vol. 186, pp. 91–99, Feb. 2015.

[4] D.-S. Xu, L.-J. Dong, L. Borana, and H.-B. Liu, "Early–warning system with quasi–distributed fiber optic sensor networks and cloud computing for soil slopes," *IEEE Access*, vol. 5, pp. 25437–25444, 2017.

[5] Y. Xing, J. Yue, C. Chen, K. Cong, S. Zhu, and Y. Bian, "Dynamic displacement forecasting of Dashuitian landslide in China using variational mode decomposition and stack long short–term memory network," *Appl. Sci.*, vol. 9, no. 15, p. 2951, Jul. 2019.

[6] C. Lian, L. Zhu, Z. Zeng, Y. Su, W. Yao, and H. Tang, "Constructing prediction intervals for landslide displacement using bootstrapping random vector functional link networks selective ensemble with neural networks switched," *Neurocomputing*, vol. 291, pp. 1–10, May 2018.

[7] S. Miao, X. Hao, X. Guo, Z. Wang, and M. Liang, "Displacement and landslide forecast based on an improved version of Saito's method together with the Verhulst-Grey model," *Arabian J. Geosci.*, vol. 10, no. 3, p. 53, Feb. 2017.

IEEE Access

Y. Xing *et al.*: Interval Estimation of Landslide Displacement Prediction Based on Time Series Decomposition and LSTM Network

[8] K. G. Li, J. Xu, and G. Y. Huang, "Prediction for slope displacement based on unequal interval GM (1, 1) model," *Chin. J. Underground Space Eng.*, vol. 2, no. 6, pp. 988–992, Dec. 2006.

[9] F. Huang, J. Huang, S. Jiang, and C. Zhou, "Landslide displacement prediction based on multivariate chaotic model and extreme learning machine," *Eng. Geol.*, vol. 218, pp. 173–186, Feb. 2017.

[10] J. Du, K. Yin, and S. Lacasse, "Displacement prediction in colluvial landslides, Three Gorges Reservoir, China," *Landslides*, vol. 10, no. 2, pp. 203–218, Apr. 2013.

[11] F. Miao, Y. Wu, Y. Xie, and Y. Li, "Prediction of landslide displacement with step-like behavior based on multialgorithm optimization and a support vector regression model," *Landslides*, vol. 15, no. 3, pp. 475–488, Mar. 2018.

[12] C. Zhou, K. Yin, Y. Cao, E. Intrieri, B. Ahmed, and F. Catani, "Displacement prediction of step-like landslide by applying a novel kernel extreme learning machine method," *Landslides*, vol. 15, no. 11, pp. 2211–2225, Nov. 2018.

[13] Y. Zhang, X. Wang, and H. Tang, "An improved Elman neural network with piecewise weighted gradient for time series prediction," *Neurocomputing*, vol. 359, pp. 199–208, Sep. 2019.

[14] H. Wang and L. Wang, "Modeling temporal dynamics and spatial configurations of actions using two-stream recurrent neural networks," in *Proc. IEEE Conf. Comput. Vis. Pattern Recognit.*, Honolulu, HI, USA, Jul. 2017, pp. 499–508.

[15] B. Krause, E. Kahembwe, I. Murray, and S. Renals, "Dynamic evaluation of neural sequence models," 2017, *arXiv:1709.07432*. [Online]. Available: https://arxiv.org/abs/1709.07432

[16] J. Chung, K. Kastner, L. Dinh, K. Goel, A. C. Courville, and Y. Bengio, "A recurrent latent variable model for sequential data," in *Advances in Neural Information Processing Systems*. Cambridge, MA, USA: MIT Press, 2015, pp. 2980–2988.

[17] H. Strobelt, S. Gehrmann, H. Pfister, and A. M. Rush, "LSTMVis: A tool for visual analysis of hidden state dynamics in recurrent neural networks," *IEEE Trans. Vis. Comput. Graph.*, vol. 24, no. 1, pp. 667–676, Jan. 2018.

[18] W. Xue, I. B. Nachum, S. Pandey, J. Warrington, S. Leung, and S. Li, "Direct estimation of regional wall thicknesses via residual recurrent neural network," in *Proc. Int. Conf. Inf. Process. Med. Imag.* Cham, Switzerland: Springer, 2017, pp. 505–516.

[19] P. Bashivan, I. Rish, M. Yeasin, and N. Codella, "Learning representations from EEG with deep recurrent convolutional neural networks," 2015, *arXiv:1511.06448*. [Online]. Available: https://arxiv.org/abs/1511.06448

[20] P. Coulibaly and C. K. Baldwin, "Nonstationary hydrological time series forecasting using nonlinear dynamic methods," *J. Hydrol.*, vol. 307, nos. 1–4, pp. 164–174, Jun. 2005.

[21] S. Hochreiter and J. Schmidhuber, "Long short-term memory," *Neural Comput.*, vol. 9, no. 8, pp. 1735–1780, 1997.

[22] C. Wang, N. Lu, S. Wang, Y. Cheng, and B. Jiang, "Dynamic long short-term memory neural-network-based indirect remaining-useful-life prognosis for satellite lithium-ion battery," *Appl. Sci.*, vol. 8, no. 11, p. 2078, Oct. 2018.

[23] S. Xu and R. Niu, "Displacement prediction of Baijiabao landslide based on empirical mode decomposition and long short-term memory neural network in Three Gorges area, China," *Comput. Geosci.*, vol. 111, pp. 87–96, Feb. 2018.

[24] P. Xie, A. Zhou, and B. Chai, "The application of long short–term memory(LSTM) method on displacement prediction of multifactor–induced landslides," *IEEE Access*, vol. 7, pp. 54305–54311, 2019.

[25] D. Kingma and J. L. Ba, "Adam: A method for stochastic optimization," 2014, *arXiv:1412.6980*. [Online]. Available: https://arxiv.org/abs/1412.6980

[26] A. N. Tikhonov, "On the stability of inverse problems," *Dolklady Akademii Nauk SSSR*, vol. 39, no. 5, pp. 195–198, Jan. 1943.

[27] J. Wang, Z. Sun, Z. Yu, and X. Chai, "Remaining useful life interval estimation for machine parts based on SVM," *J. Northeastern Univ. (Natural Sci.)*, vol. 37, no. 7, pp. 974–978, Jul. 2016.

[28] J. Ma, H. Tang, X. Liu, T. Wen, J. Zhang, Q. Tan, and Z. Fan, "Probabilistic forecasting of landslide displacement accounting for epistemic uncertainty: A case study in the three gorges reservoir area, China," *Landslides*, vol. 15, no. 6, pp. 1145–1153, Jun. 2018.

[29] C. Lian, Z. Zeng, W. Yao, and H. Tang, "Ensemble of extreme learning machine for landslide displacement prediction based on time series analysis," *Neural Comput. Appl.*, vol. 24, no. 1, pp. 99–107, Jan. 2014.

[30] C. Zhou, K. Yin, Y. Cao, B. Ahmed, and X. Fu, "A novel method for landslide displacement prediction by integrating advanced computational intelligence algorithms," *Sci. Rep.*, vol. 8, no. 1, p. 7287, Dec. 2018.

[31] C. Lian, Z. Zeng, W. Yao, and H. Tang, "Extreme learning machine for the displacement prediction of landslide under rainfall and reservoir level," *Stochastic Environ. Res. Risk Assessment*, vol. 28, no. 8, pp. 1957–1972, Dec. 2014.

[32] N. Ambraseys and M. Srbulov, "Earthquake induced displacements of slopes," *Soil Dyn. Earthquake Eng.*, vol. 14, no. 1, pp. 59–71, Jan. 1995.

[33] C. A. Stamatopoulos, "Limit sliding-block seismic displacement for landslide triggering along slip surfaces consisting of saturated sand," *Soil Dyn. Earthquake Eng.*, vol. 79, pp. 265–277, Dec. 2015.

[34] T. E. Tika and J. N. Hutchinson, "Ring shear tests on soil from the Vaiont landslide slip surface," *Géotechnique*, vol. 49, no. 1, pp. 59–74, Feb. 1999.

[35] C. A. Stamatopoulos and B. Di, "Analytical and approximate expressions predicting post-failure landslide displacement using the multi-block model and energy methods," *Landslides*, vol. 12, no. 6, pp. 1207–1213, Dec. 2015.

[36] B. Yang, K. Yin, T. Xiao, L. Chen, and J. Du, "Annual variation of landslide stability under the effect of water level fluctuation and rainfall in the Three Gorges Reservoir, China," *Environ. Earth Sci*, vol. 76, no. 16, pp. 564–580, Aug. 2017.

[37] B. Yang, K. Yin, S. Lacasse, and Z. Liu, "Time series analysis and long short-term memory neural network to predict landslide displacement," *Landslides*, vol. 16, no. 4, pp. 677–694, Apr. 2019.

[38] T. Glade, M. Anderson, and M. J. Crozier, *Landslide Hazard and Risk*. Vienna, Austria: Wiley, vol. 2012, pp. 1–40.

[39] L. Li, Y. Wu, F. Miao, K. Liao, and L. Zhang, "Displacement prediction of landslides based on variational mode decomposition and GWO-MIC-SVR model," *Chin. J. Rock Mech. Eng.*, vol. 37, no. 6, pp. 1395–1406, Apr. 2018.

**YIN XING** was born in 1992. She received the M.S. degree in surveying and mapping engineering from the Guilin University of Technology, Guangxi, China, in 2018. She is currently pursuing the Ph.D. degree in geodesy and surveying engineering with the School of Earth Sciences and Engineering, Hohai University. Her current research interest includes monitoring and prediction of landslide displacement.

**JIANPING YUE** was born in 1963. He received the Ph.D. degree from Hohai University, Nanjing, China. He is currently a Full Professor with the School of Earth Sciences and Engineering, Hohai University. His current research interests include geodetic surveying, precision engineering surveying, and safety monitoring. He has been awarded by many national activities.

**CHUANG CHEN** was born in 1992. He received the M.S. degree in control engineering from Nanjing Tech University, Nanjing, China, in 2018. He is currently pursuing the Ph.D. degree in control theory and control engineering with the College of Automation Engineering, Nanjing University of Aeronautics and Astronautics. His current research interests include stochastic modeling of systems degradation, performance evaluation, and optimization of dynamic maintenance strategies.

● ● ●